keV fullerene interaction with hydrocarbon targets: Projectile penetration, damage creation and removal

Arnaud Delcorte [a,*], Barbara J. Garrison [b]

[a] *PCPM Laboratory, Université catholique de Louvain, Croix du Sud 1, B-1348 Louvain-la-Neuve, Belgium*
[b] *Chemistry Department, The Pennsylvania State University, University Park, PA, USA*

Abstract

The physics of energetic fullerene projectile penetration, damage creation and sputtering in organic solids is investigated via molecular dynamics simulations. Two models are used, the first one based on a full atomistic description of the target and the second one, using a coarse-grain prescription that was recently developed and tested for a benzene molecular crystal [E. Smiley, Z. Postawa, I.A. Wojcie-chowski, N. Winograd, B. J. Garrison, Appl. Surf. Sci. 252 (2006) 6436]. The results explore the mechanism of energy transfer from the C_{60} projectile to the organic target atoms/molecules through the comparison with significantly different projectiles (Argon) and samples (Ag crystal). The effects of the projectile energy on the penetration and fast energy transfer processes (200 fs) are also delineated. The second part of the results investigates the 'long term' consequences (20–50 ps) of fullerene impacts in hydrocarbon sample surfaces. In an icosane ($C_{20}H_{42}$) solid, a 5 keV C_{60} projectile induces a crater of ∼10 nm diameter surrounded by a ∼4 nm wide rim and ejects ∼70 intact molecules. More than 75% of the fragments generated by the fullerene in the surface are also sputtered away by the end of the event. The perspective considers the capabilities of fullerene projectiles for depth profile analysis of molecular samples by particle-induced desorption mass spectrometry.
© 2006 Elsevier B.V. All rights reserved.

PACS: 79.20.Rf; 36.40.−c; 07.77.Gx; 36.20.Eg

Keywords: Sputtering; Cluster ions; Depth profiling; Molecular dynamics; ToF-SIMS; Organic materials

1. Introduction

Owing to the recent advent of reliable ion sources [1,2], buckminsterfullerenes are now used as primary projectiles for surface characterization by secondary ion mass spectrometry (SIMS). For organic material analysis, fullerene ions display several advantages in comparison with monoatomic (Ga^+, In^+, Cs^+) and even metal cluster ions such as Au_3^+. Among these properties, enhanced molecular ion yields [1,3], expanded secondary ion mass range [3], reduced damage cross-sections [1] and a reduced topography creation upon erosion of the surface [4] provide a new potential for high lateral resolution imaging of organic surfaces and even molecular depth-profiling. All of a sudden, the dream of many surface analysts, i.e. a full 3-D characterization of the molecules present in organic (multilayers, OLEDs) or biological samples (cells, tissues), does not seem to be out of reach anymore.

The physics behind these outstanding properties of fullerene projectiles started unraveling with the help of molecular dynamics simulations. The case of metal targets is now quite well understood: in contrast with monoatomic ions, 15 keV C_{60} projectiles split up in the topmost layers of the sample, inducing a collective outward motion involving hundreds of target atoms, the creation of an hemispherical crater with a surrounding rim and the massive ejection of atoms and clusters. For silver surfaces, sputtering yield enhancements of 7 (Ag), 27 (Ag_2) and 40 (Ag_3) have been predicted by the simulations [5]. A similar process occurs

* Corresponding author. Tel.: +32 10473582; fax: +32 10473452.
 E-mail address: delcorte@pcpm.ucl.ac.be (A. Delcorte).

when 1–3 molecular layers are adsorbed on the surface. In the particular case of benzene on Ag, the molecules eject from the expanding crater via a 'catapult' mechanism [6]. However, for such thin organic layers on metals, the simulations only predict a small (or no) molecular yield enhancement, which was explained by a combination of factors, including the damage created by the projectile in the overlayer and the limited amount of organic material present in the interaction volume. All these predictions agree well with recent experiments [7].

Studying the sputtering of purely organic samples by keV fullerenes ions, however, is still challenging. Indeed, the mesoscopic size of the interaction volume and the pressure pulse induced in the surface require sample sizes that are too large, and therefore trajectory computations that are too time-consuming, for full atomistic calculations. Recently, a prescription has been developed for treating larger ensembles of atoms using a coarse-grained approach [8]. This new model has already been applied to the sputtering of benzene crystals by fullerene ions and the results obtained under 500 eV C_{60} bombardment of benzene are comparable to those obtained with the atomistic model [8].

In this article, the penetration of keV fullerene projectiles in amorphous solids made of short linear hydrocarbon chains (polystyrene oligomers, icosane) and the subsequent energy transfer, damage creation and sputtering mechanisms are investigated using a combination of fully atomistic and coarse-grained MD simulations. The results suggest a reasonable explanation to the experimental observation that sample depth-profiling with the retention of molecular/characteristic fragment information is possible with C_{60} projectiles [1,4,9].

2. Simulation methods

In order to describe the time-evolution of the investigated system at the microscopic level, Hamilton's equations of motion are numerically integrated over some time interval, providing us with the position and velocity of each particle at each timestep [10]. Forces among the atoms or particles in the system are derived from semi-empirical interaction potentials whose careful choice constitutes the key of a realistic description of the studied mechanisms. In this article, two approaches are considered: in the first one, the sample is described at the atomistic level while, in the second one, certain atoms are grouped to form united atoms or particles. The advantages of such a coarse-grained approach is that there are fewer particles, the potentials are simpler thus quicker to calculate and the fast H-vibration is eliminated which allows for a larger time step to be used in the integration.

The computational cell for atomistic simulations of polystyrene samples (PS) is a box containing 36 192 atoms, forming 464 molecules (twice as large as the sample described in [11]). The PS molecules are butyl-ended tetramers (four repeat units) with a molecular weight of 559 amu (accounting for the use of ^{3}H instead of regular

H for computational efficiency). The C–C, C–H and H–H interactions are described by the AIREBO potential for both the sample relaxation and the interaction with Ar and C_{60} projectiles. The synthesis of a similar sample has been described in detail in [11].

The computational cell for coarse-grained simulations of icosane samples ($C_{20}H_{42}$) is a box containing 256 000 united atoms (793 600 atom equivalents), forming 12 800 molecules (Fig. 1). The icosane molecules are constituted of 18 CH_2 particles of 14 amu and capped with two CH_3 particles of 15 amu. The amorphous icosane sample used in the sputtering simulations was generated as follows. First, a periodic unit cell containing 50 $C_{20}H_{42}$ molecules in an amorphous arrangement was designed at the atomistic level and relaxed using the Accelrys Cerius^2 software package. This basic cell was then coarse-grained by using the position of the corresponding carbon atoms for the coordinates of the CH_2 and CH_3 united atoms. Two hundred and fifty-six of these cells were necessary to form the final sample. The obtained solid, with the united atom positions defined as described above, was far from equilibrium within the potential set used for the sputtering simulations and several stages of heating and relaxation were necessary to reach an equilibrium configuration. With the chosen potentials, the density of the relaxed icosane solid is 0.90 g/cm^3. Reported experimental values for the density of this compound vary between 0.79 and 0.93 g/cm^3 [12,13].

In the coarse-grain model, a Lennard-Jones potential is used to describe the interactions of the particles located on different molecules. The values of ε and σ have been chosen from previous studies describing linear hydrocarbons [14,15]. For the intramolecular interactions, the model must allow molecules to store internal energy up to the point when they dissociate. A Morse potential between adjacent CH_2 and CH_3 particles has been chosen to account for the dissociating bond stretch term, with parameters that reflect the bond strength and equilibrium distance in linear hydrocarbons [14,15]. The other interactions are between CH_x particles separated by one CH_x particle, which are modeled by a Morse potential with a small well depth [8]. This pair potential allows the particles to interact if the molecule is dissociated and also provide an equilibrium configuration of the sample in which the molecules adopt the appropriate zig–zag shape. This type of interaction has been preferred to an angle bend term that does not allow for dissociation and is therefore limiting for sputtering simulations. The potential parameters are summarized in Table 1. In all the simulations, the AIREBO potential is used to describe the C–C interaction of the C_{60} projectile [2]. In the coarse-grain model, a weak Lennard-Jones potential is used between the C atoms of the fullerene and the CH_x particles of the molecular sample (see Table 1).

3. Fullerene penetration in an organic surface

The penetration of a fullerene projectile in a polystyrene oligomer sample has been studied via full atomistic MD
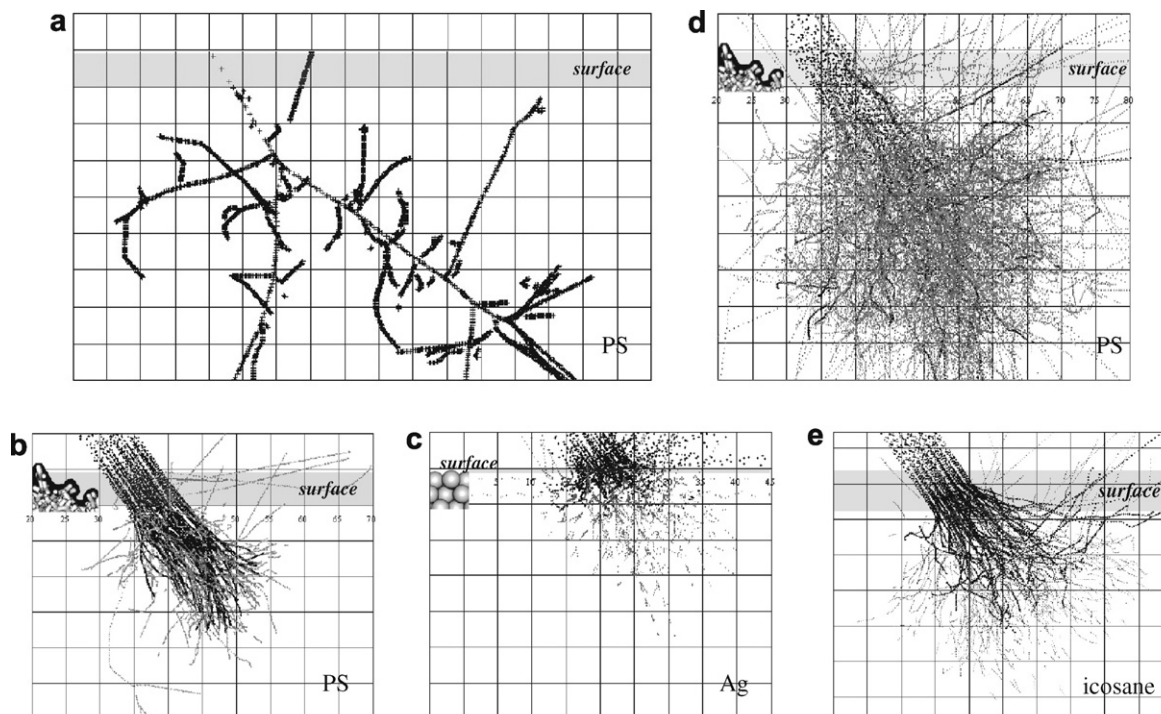
Fig. 1. Tracks of the atoms forming the collision cascade in a polystyrene tetramer (a, b, d), in a silver crystal (c) and in an icosane (e) solid. The successive positions of the projectile and recoil atoms with more than 10 eV of kinetic energy are represented as a function of time up to 200 fs. Each square of the grid is 5×5 Å^2. The sample-vacuum interface is indicated by the grey area. (a) Ar $\rightarrow$ PS, 5 keV; (b) $C_{60} \rightarrow$ PS, 5 keV; (c) $C_{60} \rightarrow$ Ag{111}, 5 keV; (d) $C_{60} \rightarrow$ PS, 25 keV; (e) $C_{60} \rightarrow$ icosane, 5 keV, coarse-grained model.

Table 1
Morse[a] and Lennard-Jones[b] interaction parameters

	D_e (eV)	r_e (Å)	α	r_{cutoff} (Å)
Morse				
CH$_2$–CH$_2$				
1–2	3.6	1.53	2	5.0
1–3	0.01	2.52	2	5.0
CH$_2$–CH$_3$				
1–2	3.6	1.53	2	5.0
1–3	0.01	2.52	2	5.0
	ε (eV)	σ (Å)		r_{cutoff} (Å)
Lennard-Jones				
C–CH$_2$, C–CH$_3$	0.0040	3.70		7.65
CH$_2$–CH$_2$	0.0052	3.85		7.65
CH$_2$–CH$_3$	0.0062	3.91		7.65
CH$_3$–CH$_3$	0.0076	3.91		7.65

[a] The 1–2 interactions are defined as the nearest neighbor interactions and the 1–3 are the next nearest neighbor interactions.
[b] A 12–6 Lennard-Jones potential is used.

simulations. This part of the interaction covers the first 150–200 fs of the trajectories and precedes any pressure pulse or collective outward motion that could develop beyond the range of the fast moving atoms resulting from bond breaking in the sample. Therefore, within this time range, a relatively small target is sufficient to contain the action and the calculation is tractable with atomistic simulations even for relatively large projectile energies (25 keV

or more). Fig. 1 gives an overview of the projectile penetration as a function of the projectile nature (Fig. 1(a) and (b)), the target nature (Fig. 1(b) and (c)), the fullerene kinetic energy (Fig. 1(b) and (d)) and the chosen model (Fig. 1(b) and (e)). The incidence angle is 45° in all cases and the scale of the figures is such that a direct visual comparison is possible.

The comparison between 5 keV Ar and C_{60} projectiles (Fig. 1(a) and (b)) impinging polystyrene shows several effects. First, Ar penetrates much farther than C_{60} in the organic sample. In this trajectory, it exits through the side of the sample with a remaining kinetic energy of about 0.5 keV. The projectile creates several bond-scissions and a cascade of collisions extending in the depth of the sample. Only a few branches of this cascade are upward directed, i.e. the quantity of energy available for surface molecular ejection is only a fraction of the projectile energy. In comparison, the C_{60} projectile stops in the top 20 Å of the target and the displaced atoms remain in a radius of 10–15 Å. The projectile dissociates but the lateral straggling between the C constituents, after the slowing down of the fullerene, is low. Overall, the action is confined in a much smaller volume. On the other hand, the overlapping atom tracks, as well as the details of the energy transfer over the considered time frame show that the energy density in the interaction volume at 200 fs is much larger with C_{60}.

As was the case for monoatomic projectiles, the C_{60} projectile penetration is strongly influenced by the average

atomic mass (metals versus organics) and by the microscopic structure of the sample (opening of the lattice). This effect is obvious when the bombardment of a polystyrene target is compared to that of a Ag{111} target (Fig. 1(c)). In the case of the heavy, close-packed silver crystal, the fullerene does not penetrate deeper than the top 5 Å of the surface and a large number of carbon atoms are directly backscattered. However, there is a similarity with the polystyrene case in that the geometry of the displaced atom volume also exhibits a spherical symmetry, unlike the case of Ar bombardment. A few pairs of simultaneous focused collision sequences suggest the collective nature of the projectile-target interaction even at this early stage of the trajectories. This collective motion, almost mesoscopic, has been investigated in detail by other authors [5].

When the kinetic energy of the fullerene projectile increases, from 5 keV to 25 keV, the penetration depth and the lateral straggling of the C atoms are larger and the size of the interaction volume increases significantly. Fig. 1(d) indicates that the atoms displaced within the first 200 fs are confined in a spherical volume with a radius of about 20–25 Å. The increase of the interaction volume roughly reflects the increase of the projectile energy from 5 to 25 keV (a factor of 5). Therefore, the energy density

in the disturbed volume after 200 fs is not significantly different.

Fig. 1(e) shows a similar picture but for the 5 keV C_{60} bombardment of icosane ($C_{20}H_{42}$) within the coarse-grained model. The pattern of atom tracks of Fig. 1(e) resembles the one described at the atomistic level for polystyrene (Fig. 1(b)). The geometry of the interaction volume is still spherical and its size is comparable. Nevertheless, there are some differences. First, the C constituent atoms of the fullerene projectile tend to deviate more from their initial trajectory and they "implant" slightly closer to the surface (grey area). Second, more recoil atoms are created in the solid as a result of the interaction with the projectile. Beyond the specific nature and molecular structure of the samples (PS versus icosane), there might be some influence of the system description (atomistic versus coarse-grained) on the results. First, the potentials are different and the H atoms, supposed to offer less resistance to the projectile penetration, are not explicitly present in the icosane system. Second, the "atomistic" PS target has more bonds to internally store energy than the "coarse-grained" icosane, leaving somewhat less energy for bond-scissions and recoil atom creations in the PS system. A rigorous investigation of such effects will be carried out using the same sample with both models. Despite the observed differences, we feel
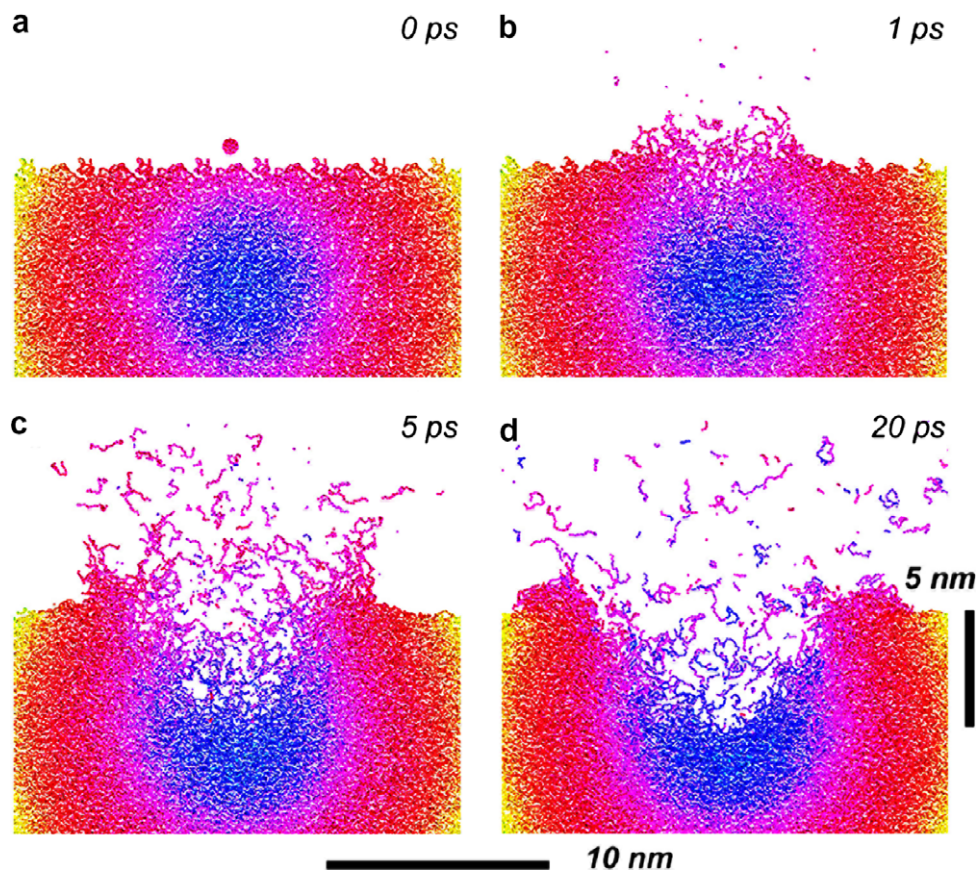

Fig. 2. Snapshots showing the time-evolution of the molecular dynamics for an icosane molecular solid under 5 keV C_{60} bombardment (normal incidence). Only a 60 Å thick slab cut around the impact point of the projectile is represented in order to show the details of the crater formation. The sample particles are radially colored from blue to yellow going outwards from the center of sample. (For interpretation of the references in colour in this figure legend, the reader is referred to the web version of this article.)

confident that the coarse-grained model is retaining the essential physics of the projectile penetration and the subsequent dynamics of the energized volume, as explained in the next section.

4. Collective motion and crater formation

Fig. 2 describes the time-evolution of a trajectory for the 5 keV C_{60} bombardment of icosane in the coarse-grained model. The incidence is normal. The images only show a 6 nm thick slab of the sample in order to emphasize the collective motion and crater formation around the impact of the projectile in the sample. After the penetration of the fullerene constituent atoms, within the first 200 fs (see Fig. 1), the high energy density in the interaction volume generates a collective outward motion, qualitatively similar to the C_{60} bombardment of silver and benzene crystals [8]. The emission process really starts between 500 fs and 1 ps, with the release of relatively fast atoms and fragments from the energized volume (Fig. 2(b)). Afterwards, this nanovolume expands into the vacuum, creating a plume of upward moving fragments, intact molecules and large molecular clusters (Fig. 2(c)–(d)). The color coding indicates that a significant fraction of the emitted molecules and fragments (blue) originate in the depth of the forming crater. The observed mechanism is reminiscent of the jet flow or adiabatic expansion into the vacuum described by several authors for the case of frozen gases under keV monoatomic projectile bombardment [16] and, on a smaller scale, of the plume expansion monitored in laser ablation simulations [17].

The outward expansion first triggered by the fast moving atoms (Fig. 1) eventually generates a crater surrounded by a 10–15 Å high rim made of molecules pushed away during the process but whose center-of-mass kinetic energy was insufficient for desorption. After 20 ps, the diameter of the crater (at the level of the original surface) is close to 10 nm and the width of the annular rim, about 4 nm. Fig. 1(b) and (d) and the results obtained with silver crystals [5] suggest that the crater size is significantly dependent on the projectile energy.

In this specific trajectory, 69 intact molecules, 305 fragments (among which 202 CH_2 united atoms) and six noncovalent clusters containing 2–6 icosane molecules are ejected. A statistical analysis involving ten such trajectories indicates that the average yield (number of sputtered species per projectile) is 380 and the yield variation does not exceed 6% (standard deviation). A similar conclusion, at odds with monoatomic projectile bombardment results, could also be drawn for the C_{60} bombardment of benzene adsorbed on silver crystals [18].

5. Damage creation and removal

The impinging fullerene projectile generates a significant amount of damage in the surface, via direct bond-scissions (Fig. 1) and, perhaps, other delayed degradation

mechanisms. One way to investigate the damage created in the icosane sample surface upon bombardment is to monitor the quantity of 'radicals' formed in the target in the course of the projectile penetration and energy dissipation stages of the interaction. In this article, radicals are defined as CH_x united atoms being initially part of an icosane molecule and whose bonds with the rest of the molecule are severed at some point in time as a result of energy transfer from the projectile or from other recoil atoms (other radicals). Considering the icosane sample, CH_2 particles can either have one or two bonds broken while CH_3 particles can only have one bond broken. The created radicals can therefore be single CH_x particles or any type of 'molecular' fragment resulting from bond-scissions in the icosane molecule. The amount of radicals generated in the sample is reported in Fig. 3(a) as a function of time. It is split in two families, the first one corresponding to radicals located in the sample surface (full triangles) and the second one, to radicals located above the sample surface (i.e. ejected). First, the results indicate that radicals are still generated after the extinction of the 'collision cascade' described in Fig. 1, as a result of the internal energy stored in the molecules which undergo delayed decomposition. The maximum of the number of radicals present in the sample spreads over a time span of about half a
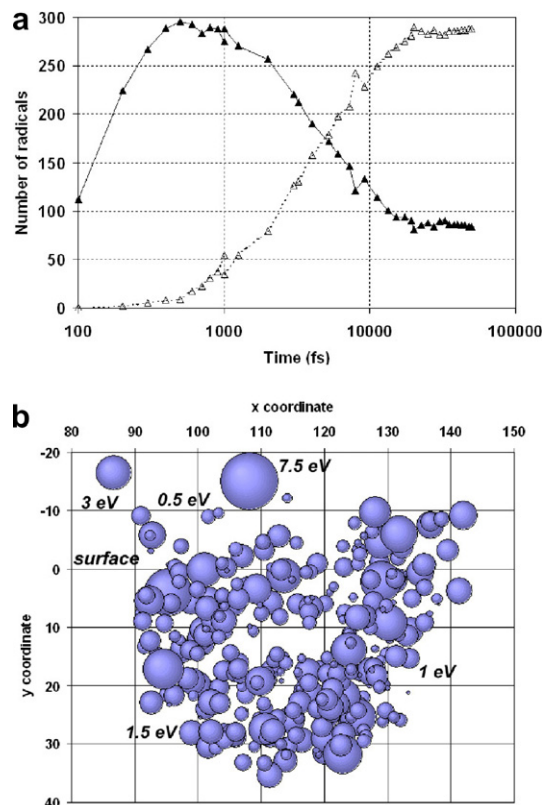

Fig. 3. (a) Time-evolution of the number of radicals created in an icosane target by a 5 keV C_{60} projectile (normal incidence). *Full triangles:* radicals present in the sample surface; *Open triangles:* radicals ejected from the solid. (b) Positions and kinetic energy (projected area of the spheres) of the radicals at 500 fs. Each square of the grid is 10×10 Å^2.

picosecond, between 500 fs and 1 ps after the impact of the projectile. The $\sim$300 radicals present at 500 fs in the solid correspond to 44 fragmented molecules. Some of the icosane molecules undergo more than 10 bond-scissions while others are broken in only one point. The number of radicals decreases afterwards, because more and more fragments desorb from the sample surface. The entire process of radical creation/emission extends over a period of 20 ps. In the end, more than 75% of those fragments are sputtered in the vacuum, leaving less than 25% of the damage in the sample surface. A topological study of the radical positions as a function of time indicates that they mostly arise from the center of the developing crater and follow the general outward/upward motion depicted in Fig. 2. Fig. 3(b) shows a side view of the situation around the maximum of the full curve of Fig. 3(a) (500 fs). Each sphere represents a radical and the size of the spheres is proportional to their kinetic energy, mostly comprised between 0.1 eV and 5 eV. At this time, many radicals are located on the expanding crater edges and in the upward moving central volume. The combination of Figs. 2 and 3 helps understand how most of these fragments are eventually released in the vacuum.

6. Conclusion and perspective

According to our MD simulations, 5 keV fullerene projectiles are stopped in the topmost layers of molecular samples such as polystyrene oligomers and icosane ($C_{20}H_{42}$). Bond-scissions and damage creation do not occur in the depth of the sample and the fragmented molecules originate from a hemispherical nanovolume that ends up being devoid of material when the crater is fully formed. As a result, a large fraction of these fragments (>75%) are sputtered away by the fullerene projectile. In contrast, keV monoatomic projectiles dissipate a large fraction of their energy in the sub-surface of the sample, inducing damage that remains in the solid after dissipation of the deposited energy. The consequence for surface analysis by particle-induced desorption is clear. While the continuous bombardment with monoatomic projectile leads to an accumulation of damage as a function of primary ion dose, the use of fullerene ions, immediately wiping out a large fraction of the created fragments, should allow to keep – at least a fraction of the molecular information upon depth profiling. Experimental results involving the fullerene bombardment of relatively small organic molecules (below 10 kDa) seem to agree with this conclusion drawn from the simulations [1,4]. The case of larger molecules such as proteins and high-molecular weight polymers, however, is less clear. While depth-profiling of poly(methyl methacrylate) (a polymer that is well-known for unzipping under irradiation) could be achieved using SF_5^+ [19] and C_{60}^+ [20] ions, the same is not true for polystyrene [20,21]. We speculate that, because of their entangled structure, sputtering from such samples might be less extensive and the remaining damage, still able to induce classical degradation reac-

tions like dehydrogenation, preferential pendant group elimination, branching and cross-linking that could scramble the desired molecular information.

Acknowledgements

References

[1] D.E. Weibel, S. Wong, N. Lockyer, P. Blenkinsopp, R. Hill, J.C. Vickerman, Anal. Chem. 75 (2003) 1754.

[2] F. Kollmer, Appl. Surf. Sci. 231–232 (2004) 153.

[3] A. Delcorte, C. Poleunis, P. Bertrand, Appl. Surf. Sci. 252 (2006) 6494.

[4] N. Winograd, Anal. Chem. 77 (2005) 143A.

[5] Z. Postawa, B. Czerwinski, M. Szewczyk, E.J. Smiley, N. Winograd, B. Garrison, J. Phys. Chem. 108 (2004) 7831.

[6] Z. Postawa, B. Czerwinski, N. Winograd, B.J. Garrison, J. Phys. Chem. B 109 (2005) 11973.

[7] S. Sun, C. Szakal, E.J. Smiley, Z. Postawa, A. Wucher, B.J. Garrison, N. Winograd, Appl. Surf. Sci. 231–232 (2004) 64.

[8] E. Smiley, Z. Postawa, I.A. Wojciechowski, N. Winograd, B.J. Garrison, Appl. Surf. Sci. 252 (2006) 6436.

[9] J. Cheng, A. Wucher, N. Winograd, J. Phys. Chem. B 110 (2006) 8329.

[10] B.J. Garrison, in: J.-C. Vickerman, D. Briggs (Eds.), ToF-SIMS: Surface analysis by mass spectrometry, SurfaceSpectra/IMPublications, Chichester, 2001, p. 223.

[11] A. Delcorte, B.J. Garrison, J. Phys. Chem. B 108 (2004) 15652.

[12] <http://physchem.ox.ac.uk/MSDS/EI/eicosane.html>.

[13] <http://www.chem007.com/specification_d/chemicals/supplier/cas/n-Eicosane.asp>.

[14] J. Hautman, M.L. Klein, J. Chem. Phys. 91 (1989) 4994.

[15] S. Balasubramanian, M.L. Klein, J.I. Siepmann, J. Chem. Phys. 103 (1995) 3184.

[16] C.T. Reimann, in: P. Sigmund (Ed.), Fundamental Processes in Sputtering of Atoms and Molecules, Copenhagen, Mat. Fys. Medd. 43 (1993) 351, and references therein.

[17] L.V. Zhigilei, E. Leveugle, B.J. Garrison, Y.G. Yingling, M.I. Zeifman, Chem. Rev. 103 (2003) 321.

[18] B. Czerwinski, R. Samson, B.J. Garrison, N. Winograd, Z. Postawa, Vacuum 81 (2006) 167.

[19] G. Gillen, S. Roberson, Rapid Commun. Mass Spectrom. 12 (1998) 1303.

[20] R. Möllers, N. Tuccitto, V. Torrisi, E. Niehuis, A. Licciardello, Appl. Surf. Sci. 252 (2006) 6509.

[21] D.E. Weibel, N. Lockyer, J.C. Vickerman, Appl. Surf. Sci. 231–232 (2004) 146.